Note di Matematica
Note Mat. **32** (2012) n. 1, 63–85.
ISSN 1123-2536, e-ISSN 1590-0932
doi:10.1285/i15900932v32n1p63

Modeling and Simulation of Thick Sprays through Coupling of a Finite Volume Euler Equation Solver and a Particle Method for a Disperse Phase

S. Benjelloun
CMLA, ENS Cachan, PRES UniverSud,
61 av du Président Wilson, 94235, Cachan, Cedex, France

L. Desvillettes
CMLA, ENS Cachan & IUF, PRES UniverSud,
61 av du Président Wilson, 94235, Cachan, Cedex, France.

J.M. Ghidaglia
CMLA, ENS Cachan, PRES UniverSud,
61 av du Président Wilson, 94235, Cachan, Cedex, France

K. Nielsen
Engineering Research & Development Department, ENI E&P Division,
via Emilia 1, I-20097 San Donato Milanese (Mi), Italy.

Abstract. We present here the principles of the coupling between an efficient numerical method for hyperbolic systems, namely the FVCF scheme (that is, a finite volume scheme used in the context of non conservative equations arising in multiphase flows), on the one hand; and a particle method for the Vlasov-Boltzmann equation of PIC-DSMC type (that is, in which macroscopic quantities are computed in each cell by adding quantities attached to the particles, and where integrals are computed thanks to a random sampling), on the other hand.

Numerical results illustrating this coupling are shown for a problem involving a spray (droplets inside an underlying gas) in a pipe which is modeled by a 1D fluid-kinetic system.

1 Introduction

Sprays are complex flows which are constituted of an underlying gas in which a population of droplets or dust specks are dispersed, cf. [17]. There are various possibilities for modeling such flows cf. [7]; we wish here to focus on the case where the droplets are quite small (w.r.t. a characteristic length of the domain which is studied) but occupy a non negligible volume fraction of this domain (typically between 10^{-3} and 10^{-1}). In such a situation (in which the spray is sometimes called thick, cf. [17]), it is not possible to use a microscopic modeling

(in which the shape of each droplet is computed), cf. [7], and one is led to use a statistical description of the disperse phase. It is then possible to model the spray by Eulerian-Lagrangian systems (cf. [17], [18]) or Eulerian-Eulerian systems (cf. [8], [13]): we focus in this work on a typical Eulerian-Lagrangian system (described below).

Assuming (for the sake of simplicity) that the underlying gas follows the isentropic Euler's equations for compressible ideal flows, we now write the equations satisfied by the spray. Denoting by $\alpha := \alpha(t,x) \geq 0$, $\rho := \rho(t,x) \geq 0$, $u := u(t,x) \in \mathbf{R}^3$, $p := p(t,x) \geq 0$ the respective volume fraction, density, velocity and pressure of the gas at time $t > 0$ and point $x \in \mathbf{R}^3$, and by $f := f(t,x,v,r) \geq 0$ the density in the phase space of the droplets (at time t, point x) of velocity $v \in \mathbf{R}^3$ and radius $r > 0$, we end up with the system (cf. [4] for example):
Conservation of mass for the gas:

$$\partial_t(\alpha\,\rho) + \nabla_x \cdot (\alpha\,\rho\,u) = 0; \tag{1}$$

Balance of momentum for the gas

$$\partial_t(\alpha\,\rho\,u_i) + \nabla_x \cdot (\alpha\,\rho\,u \otimes u) + \nabla_x p = -\int_{v\in\mathbf{R}^3}\int_{r\in\mathbf{R}_+} f\,F\,dr dv + \alpha\,\rho\,g; \tag{2}$$

Balance of mass and momentum for the droplets:

$$\partial_t f + v\cdot\nabla_x f + \nabla_v \cdot \left(f\left[\frac{F}{\frac{4}{3}\,\rho_l\,\pi\,r^3} - |g|\begin{pmatrix}0\\1\\0\end{pmatrix}\right]\right) = Q(f); \tag{3}$$

Conservation of total volume:

$$1-\alpha = \int_{v\in\mathbf{R}^3}\int_{r\in\mathbf{R}_+} f\,\frac{4}{3}\,\pi\,r^3\,dr dv; \tag{4}$$

Pressure law of the gas (for some constants $C_0, \gamma > 0$):

$$p = C_0\,\rho^\gamma. \tag{5}$$

In these equations, g is the acceleration of the gravity, ρ_l is the density of the droplets, and $F = (F_1, F_2, F_3)$ is the force received by a droplet from the gas:

$$F = \mathcal{F}(\rho, r, |u-v|)\,(u-v) - \frac{4}{3}\,\pi\,r^3\,\nabla_x p, \tag{6}$$

where $\mathcal{F}$ is a function given in a semi-empirical way (cf. [17] for example).

Finally, Q is a collision operator between droplets which reads:

$$Q(f)(t,x,v,r) = \int_{v*\in\mathbf{R}^3}\int_{r*\in\mathbf{R}_+}\int_{\theta=0}^{\pi}\int_{\phi=0}^{2\pi}\Big(f(t,x,v',r)\,f(t,x,v^{*'},r^*) \\ -f(t,x,v,r)\,f(t,x,v^*,r^*)\Big)\,B(\theta,|v-v^*|,r,r^*)\,d\theta d\phi dr^* dv^*, \tag{7}$$

where ingoing and outgoing velocities are related by the formulas

$$\begin{aligned} v' &= \frac{r^{*3}v^* + r^3 v}{r^{*3}+r^3} + \frac{r^{*3}}{r^{*3}+r^3}\,|v-v^*|\,\sigma, \\ v^{*'} &= \frac{r^{*3}v^* + r^3 v}{r^{*3}+r^3} - \frac{r^{3}}{r^{*3}+r^3}\,|v-v^*|\,\sigma, \end{aligned} \tag{8}$$

and $\sigma \in \mathcal{S}^2$ is a unit vector parameterized by two angles $\theta \in [0,\pi]$ and $\phi \in [0,2\pi]$.

Finally, the cross section appearing in definition (7) corresponds to hard spheres collisions:

$$B := B(\theta,|v-v^*|,r,r^*) = |v-v^*|\,(r+r^*)^2\,\frac{\sin\theta}{4}. \tag{9}$$

We recall in a short list the notations used in eq. (1) – (9):

$t > 0$	time variable
$x \in \mathbf{R}^3$	space variable
$v \in \mathbf{R}^3$	velocity of a droplet
$r > 0$	radius of a droplet
$\alpha := \alpha(t,x) \in [0,1]$	volume fraction of the gas
$\rho := \rho(t,x) \geq 0$	density of the gas
$u := u(t,x) \in \mathbf{R}^3$	velocity of the gas
$p := p(t,x) \geq 0$	pressure of the gas
$g \in \mathbf{R}^3$	acceleration of gravity
$f := f(t,x,v,r) \geq 0$	density of droplets
$F := F(t,x,v,r) \in \mathbf{R}^3$	drag force
$Q := Q(f) \in \mathbf{R}$	collision kernel
$C_0, \gamma > 0$	parameters in the pressure law
$B \geq 0$	collision cross section
$v_*, v', v'_* \in \mathbf{R}^3$	velocities of droplets before and after a collision
$r_* > 0$	radius of a partner droplet in a collision
$\sigma \in S^2, \theta \in [0,\pi]$	angular parameters in a collision

Note that the Euler equations for the gas and the Vlasov-Boltzmann equation for the disperse phase are coupled through the drag force (6) on the one side, and the volume fraction α on the other side: this is typical of thick sprays.

Though no rigorous mathematical theory has yet been developed for thick sprays equations such as (1) – (9), local in time existence and uniqueness was proven for simplified models: namely for so called thin sprays (cf. [3]) and moderately thick sprays (cf. [16]).

A large variety of schemes exists for solving the compressible Euler equation (or, more generally, systems of conservation laws and balance laws, cf. [9], [14] for example). Some of them can be extended in order to include nonconservative terms or lack of hyperbolicity which are typical of multiphase flows modeled by Eulerian-Eulerian systems. Recently, a family of schemes called FVCF (Finite Volume with Characteristic Flux) has shown its efficiency for such flows (cf. [10], [11]). Our objective here is to extend the use of these FVCF schemes to the context of (thick) sprays modeled by Eulerian-Lagrangian systems such as (1) – (9), by coupling them to a particle method of PIC-DSMC type for the kinetic equation (3). Here PIC (Particles In Cells) means that quantities such as α are computed in each cell by adding quantities attached to each particle belonging to the corresponding cell (cf. [12] for example), and DSMC (Direct Simulation Monte Carlo) means that the integrals in the collision kernel Q are computed by a Monte Carlo method (cf. [5] for example).

This paper is structured as follows: In section 2, we write a 1D version of eq. (1) – (9), in order to get a suitable model for testing the behavior of our numerical method. Then, section 3 is devoted to the presentation of the numerical scheme. Finally, we give in section 4 the results of a few simulations.

2 Modeling of a spray in a pipe by 1D equations

We consider a (straight horizontal) pipe of diameter D (and section $\pi\, D^2/4$). It is represented by eq. (1) – (9) in the domain of computation $[0, L]\times B(0, D/2)$, where $B(0, D/2)$ is the disc of radius $D/2$. The axis are chosen in such a way that the vertical direction is along x_2.

It is possible to average eq. (1) – (9) along a section of the pipe, and to perform an empirical closure by imposing $u_2 = u_3 = 0$ and by identifying nonlinear functions of averages and averages of nonlinear functions. This procedure is detailed in the more complex case of a curved pipe in section 4.

After these operations, we end up with the five following equations, where $t > 0$, $x \in [0, L]$ are the time and (1D) space variables, $\rho := \rho(t, x) \geq 0$, $u := u(t, x) \in \mathbf{R}$, $\alpha := \alpha(t, x) \in [0, 1]$, $p := p(t, x) \geq 0$ are the density, velocity along the axis of the pipe, volume fraction and pressure of the gas, and $f := f(t, x, v_1, v_2, v_3, r) \geq 0$ is the density in the phase space of droplets (note that like in most 1D kinetic models, the function f still depends on a 3D velocity,

cf. [1] for example):

$$\partial_t(\alpha\,\rho) + \partial_x(\alpha\,\rho\,u) = 0; \tag{10}$$

$$\partial_t(\alpha\,\rho\,u) + \partial_x(\alpha\,\rho\,u^2) + \partial_x p = -\int_{v\in\mathbf{R}^3}\int_{r\in\mathbf{R}} f\,F_1\,dr dv; \tag{11}$$

$$\partial_t f + v_1\,\partial_x f + \nabla_v\cdot\left(f\left[\frac{F}{\frac{4}{3}\,\rho_l\,\pi\,r^3} - |g|\begin{pmatrix}0\\1\\0\end{pmatrix}\right]\right) = Q(f); \tag{12}$$

$$1-\alpha = \int_{v\in\mathbf{R}^3}\int_{r\in\mathbf{R}} f\,\frac{4}{3}\,\pi\,r^3\,dr dv; \tag{13}$$

(for some constants $C_0, \gamma > 0$)

$$p = C_0\,\rho^\gamma; \tag{14}$$

where

$$F = \mathcal{F}\left(\rho, r, \begin{vmatrix} u-v_1 \\ -v_2 \\ -v_3 \end{vmatrix}\right)\begin{pmatrix} u-v_1 \\ -v_2 \\ -v_3 \end{pmatrix} - \frac{4}{3}\,\pi\,r^3\begin{pmatrix}\partial_x p\\0\\0\end{pmatrix}, \tag{15}$$

with F still empirically given and Q still given by (7).

Note that thanks to eq. (15) and eq. (13), it is possible to rewrite eq. (11) as

$$\partial_t(\alpha\,\rho\,u) + \partial_x(\alpha\,\rho\,u^2) + \partial_x(\alpha\,p) = p\,\partial_x\alpha - \int_{v\in\mathbf{R}^3}\int_{r\in\mathbf{R}_+} f\,\mathcal{F}\begin{pmatrix} u-v_1 \\ -v_2 \\ -v_3 \end{pmatrix} dr dv. \tag{16}$$

This last formula is discretized in the next section (an empirical study shows that the direct discretization of $\alpha\,\partial_x p$ is slightly less stable).

We also introduce typical boundary conditions for both phases.

The boundary conditions are "entering" for the particles (this is the natural condition for kinetic equations when one deals with a non-physical boundary). The density of particles entering inside the tube is prescribed by two functions ψ_+ and ψ_-):

$$f(t,0,v,r) = \psi_+(t,v,r) \quad \text{for} \quad v_1 \geq 0, \tag{17}$$

$$f(t,L,v,r) = \psi_-(t,v,r) \quad \text{for} \quad v_1 \leq 0.$$

For the fluid, various boundary conditions can be imposed. The numerical computations presented in section 4 are performed in the subsonic case: the flux

of gas is prescribed on the left, and the pressure is prescribed on the right: in other words, for some value $\mathcal{G}_{in} \in \mathbf{R}$ and $p_{out} > 0$, we impose

$$\alpha(t,0)\,\rho(t,0)\,u(t,0) = \mathcal{G}_{in}; \qquad p(\rho(t,L)) = p_{out}. \tag{18}$$

Finally, the following initial data are given (for $x \in [0,L]$): the density $\rho(0,x)$ and the velocity $u(0,x)$ of the gas, the density in the phase space $f(0,x,v,r)$ of the droplets:

$$\rho(0,x) \geq 0, \qquad u(0,x) \in \mathbf{R}, \qquad f(0,x,v,r) \geq 0. \tag{19}$$

3 The numerical method

We now describe how we couple the FVCF scheme and the particle (PIC-DSMC) method in order to discretize the previous set of equations (and boundary and initial conditions), that is (10), (12) – (19).

We take a time step Δt and a space step Δx. The cells are therefore the intervals $[m\Delta x, (m+1)\Delta x[$, for $m \in \{0,..,M-1\}$ (where M is defined by $M\,\Delta x = L$).

The function f is semi-discretized (that is, discretized in space but not in time) as a sum of particles

$$f(t,x,r,v) \sim R \sum_{k=1}^{N(t)} \delta_{x_k(t),v_k(t),r_k}.$$

The numerical weight (representativity) R of the particles is fixed and the same for all particles.

The macroscopic quantities are semi-discretized through their values at the center of the cells: $\rho(t,(m+1/2)\Delta x)$, $u(t,(m+1/2)\Delta x)$, $\alpha(t,(m+1/2)\Delta x)$ and $p(t,(m+1/2)\Delta x)$.

In the framework of the time discretization, we assume that the following quantities are given at a given time $n\,\Delta t$: the total number $N(n\,\Delta t)$ of particles in the simulation; the positions, velocities and radiuses $x_k(n\,\Delta t)$, $v_k(n\,\Delta t)$, r_k of the particles, for $k = 1,..,N(n\,\Delta t)$; the macroscopic quantities $\rho(n\,\Delta t,(m+1/2)\Delta x)$, $u(n\,\Delta t,(m+1/2)\Delta x)$, $\alpha(n\,\Delta t,(m+1/2)\Delta x)$, and $p(n\,\Delta t,(m+1/2)\Delta x)$ for $m \in \{0,..,M-1\}$.

First step: (PIC method) The evolution of the quantities x_k, v_k is performed (after time discretization) through an explicit Euler scheme (we denote by $[m\Delta x,(m+1)\Delta x[$ the cell in which the particle k is located):

$$x_k((n+1)\,\Delta t) = x_k(n\,\Delta t) + \Delta t\, v_{k1}(n\,\Delta t),$$

$$v_k((n+1)\,\Delta t) = v_k(n\,\Delta t) + \Delta t \left(\frac{F}{\frac{4}{3}\,\rho_l\,\pi\,r_k^3} - |g| \begin{pmatrix} 0 \\ 1 \\ 0 \end{pmatrix} \right),$$

where

$$F = \mathcal{F}\Bigg(\rho(n\,\Delta t, (m+1/2)\Delta x), r_k, \left| \begin{array}{c} u(n\,\Delta t, (m+1/2)\Delta x) - v_{k1} \\ -v_{k2} \\ -v_{k3} \end{array} \right| \Bigg)$$

$$\times \begin{pmatrix} u(n\,\Delta t, (m+1/2)\Delta x) - v_{k1} \\ -v_{k2} \\ -v_{k3} \end{pmatrix}$$

$$-\frac{2}{3}\,\pi\,\frac{r_k^3}{\Delta x} \begin{pmatrix} (p(n\,\Delta t, (m+3/2)\Delta x) - p(n\,\Delta t, (m-1/2)\Delta x) \\ 0 \\ 0 \end{pmatrix}.$$

The last term in the force is slightly modified (un-centered) for the first and the last cell of the domain.

The particles which leave the domain of computation $[0, L]$ are eliminated, and new particles are introduced, according to the boundary conditions. We obtain in this way $N((n+1)\,\Delta t)$. Finally, at this point, the new cell in which each particle is living is computed, and the particles inside each cell are found.

Second step: (DSMC method)

The collisions (that is, the effect of $Q(f)$) are treated thanks to a standard DSMC (Discrete Simulation Monte Carlo) method, including the acceptance-rejection procedure sometimes known as "dummy collision procedure", cf. [6] and [15] for example.

Third step: The volume fraction of gas α is computed thanks to the formula

$$\alpha((n+1)\,\Delta t, (m+1/2)\Delta x) = 1 - \frac{4\,\pi\,R}{3\,\Delta x} \sum_{k \in L_m((n+1)\,\Delta t)} r_k^3,$$

where $L_m((n+1)\,\Delta t)$ is the collection of k such that $x_k((n+1)\,\Delta t) \in [m\Delta x, (m+1)\Delta x[$.

Fourth step: (FVCF scheme) We denote by

$$W_m^n := \begin{pmatrix} W_{m(1)}^n \\ W_{m(2)}^n \end{pmatrix} := \begin{pmatrix} (\alpha\,\rho)(n\,\Delta t, (m+1/2)\Delta x) \\ (\alpha\,\rho\,u)(n\,\Delta t, (m+1/2)\Delta x) \end{pmatrix}$$

the vector made up of the discretized conservative quantities.

We also introduce the flux of the fluid system (10), (11):

$$f_\alpha \begin{pmatrix} W_{(1)} \\ W_{(2)} \end{pmatrix} = \begin{pmatrix} W_{(2)} \\ W_{(2)}^2/W_{(1)} + \alpha\, p(W_{(1)}/\alpha) \end{pmatrix},$$

and its Jacobian matrix $(\partial f_\alpha/\partial W)$:

$$A_{\alpha,\rho,u} = \begin{pmatrix} 0 & 1 \\ c^2 - u^2 & 2\,u \end{pmatrix}, \tag{20}$$

where $c = \sqrt{p'(\rho)}$ is the velocity of sound. Finally we introduce the "sign" matrix

$$sgn(A_{\alpha,\rho,u}) = \begin{pmatrix} sgn(u+c)+sgn(u-c) - \frac{|u+c|-|u-c|}{2c} & \frac{sgn(u+c)-sgn(u-c)}{2c} \\ (c^2-u^2)\,\frac{sgn(u+c)-sgn(u-c)}{2c} & \frac{|u+c|-|u-c|}{2c} \end{pmatrix},$$

which is used to upwind the fluxes for the finite volume scheme.

The FVCF scheme (cf. [10], [11]), originally designed for (non necessarily conservative) balance laws, can be adapted in the following way (here α is always taken at time $(n+1)\,\Delta t$, and ρ, u at time $n\,\Delta t$).

Fourth step, first part: We begin by the convective part of the equations, without taking into account the boundary conditions (that is, $m \neq 0, M-1$).

$$\begin{aligned} W_m^{n+1/2} = W_m^n - \frac{\Delta t}{\Delta x} \Big\{ & \frac{1}{2}\,\left(f_{\alpha((m+1/2)\Delta x)}(W_m^n) + f_{\alpha((m+3/2)\Delta x)}(W_{m+1}^n)\right) \\ & -\frac{1}{2}\,sgn(A_{\alpha,\rho,u((m+1/2)\Delta x)})\,\left(f_{\alpha((m+3/2)\Delta x)}(W_{m+1}^n) - f_{\alpha((m+1/2)\Delta x)}(W_m^n)\right) \\ & -\frac{1}{2}\,\left(f_{\alpha((m-1/2)\Delta x)}(W_{m-1}^n) + f_{\alpha((m+1/2)\Delta x)}(W_m^n)\right) \\ & +\frac{1}{2}\,sgn(A_{\alpha,\rho,u((m+1/2)\Delta x)})\,\left(f_{\alpha((m+1/2)\Delta x)}(W_m^n) - f_{\alpha((m-1/2)\Delta x)}(W_{m-1}^n)\right) \Big\}. \end{aligned}$$

We obtain at this level the quantities $\rho((n+1/2)\,\Delta t, (m+1/2)\Delta x)$ and $u((n+1/2)\,\Delta t, (m+1/2)\Delta x)$, for $m \neq 0, M-1$.

The formula for $W_m^{n+1/2}$ follows the FVCF method that is Finite Volume with Characteristic Fluxes. Indeed, this method consists in using the sign matrix in order to construct a numerical flux as a linear combination of the left flux and the right flux at an interface. As said, its principle consists in upwinding along the characteristic vectors of the Jacobian matrix (20).

Fourth step, second part: The boundary conditions for the fluid are taken into account.

We introduce the left eigenvectors of $A_{\alpha,\rho,u}$ (that is, the right eigenvectors of ${}^tA_{\alpha,\rho,u}$):

$$\mathbf{l}_1 = \begin{pmatrix} -(u+c) \\ 1 \end{pmatrix}, \qquad \mathbf{l}_2 = \begin{pmatrix} -(u-c) \\ 1 \end{pmatrix}, \tag{21}$$

and its right eigenvectors (normalized in such a way that ${}^t\mathbf{l}_i\,\mathbf{r}_j = \delta_{ij}$),

$$\mathbf{r}_1 = -\frac{1}{2c}\begin{pmatrix} 1 \\ u-c \end{pmatrix}, \qquad \mathbf{r}_2 = \frac{1}{2c}\begin{pmatrix} 1 \\ u+c \end{pmatrix}. \tag{22}$$

We first perform the discretization of the left boundary condition (at $x = 0$) assuming that the flux $\alpha\,\rho\,u(0) =: \mathcal{G}_{in}$ is given.

We write down

$$W_0^{n+1/2} = W_0^n - \frac{\Delta t}{\Delta x}\Big\{ {}^t\mathbf{l}_1\,(f_{\alpha(3/2\,\Delta x)}(W_1^n) - f^-)\,\mathbf{r}_1$$

$$+ {}^t\mathbf{l}_2\,(f_{\alpha(1/2\,\Delta x)}(W_0^n) - f^-)\,\mathbf{r}_2\Big\},$$

or equivalently

$$W_0^{n+1/2} = W_0^n - \frac{\Delta t}{\Delta x}\Big\{ \frac{1}{2}\,\big(f_{\alpha(1/2\Delta x)}(W_0^n) + f_{\alpha(3/2\Delta x)}(W_1^n)\big)$$

$$-\frac{1}{2}\,sgn(A_{\alpha,\rho,u(1/2\Delta x)})\,\big(f_{\alpha(3/2\Delta x)}(W_1^n) - f_{\alpha(1/2\Delta x)}(W_0^n)\big)$$

$$-\frac{1}{2}\,\big(f^- + f_{\alpha(1/2\Delta x)}(W_0^n)\big)$$

$$+\frac{1}{2}\,sgn(A_{\alpha,\rho,u(1/2\Delta x)})\,\big(f_{\alpha(1/2\Delta x)}(W_0^n) - f^-\big)\Big\},$$

where f^- is sought under the form:

$$f^- = f_{\alpha(1/2\,\Delta x)}(W_0^n) + \varepsilon_1\,\mathbf{r}_1 + \varepsilon_2\,\mathbf{r}_2,$$

and

$${}^t\mathbf{l}_1\,f^- = {}^t\,\mathbf{l}_1\,f_{\alpha(1/2\,\Delta x)}(W_0^n), \qquad f_1^- = \mathcal{G}_{in}.$$

This leads to

$$\varepsilon_1 = 0, \qquad \varepsilon_2 = 2c\,(\mathcal{G}_{in} - f_{1;\alpha(1/2\,\Delta x)}(W_0^n)).$$

Then, we perform the discretization of the right boundary condition (at $x = L$), assuming that the pressure $p(L) =: p_{out}$ is given.

We write down

$$W_{M-1}^{n+1/2} = W_{M-1}^n - \frac{\Delta t}{\Delta x}\left\{ {}^t\mathbf{l}_1 \left(f^+ - f_{\alpha((M-1/2)\,\Delta x)}(W_{M-1}^n)\right)\mathbf{r}_1 \right.$$

$$\left. + {}^t\mathbf{l}_2 \left(f^+ - f_{\alpha((M-3/2)\,\Delta x)}(W_{M-2}^n)\right)\mathbf{r}_2 \right\},$$

or equivalently

$$W_{M-1}^{n+1/2} = W_{M-1}^n - \frac{\Delta t}{\Delta x}\left\{ \frac{1}{2}\,\left(f_{\alpha((M-1/2)\,\Delta x)}(W_{M-1}^n) + f^+\right) \right.$$

$$-\frac{1}{2}\,sgn(A_{\alpha,\rho,u((M-1/2)\,\Delta x)})\,\left(f^+ - f_{\alpha((M-1/2)\,\Delta x)}(W_{M-1}^n)\right)$$

$$-\frac{1}{2}\,\left(f_{\alpha((M-3/2)\,\Delta x)}(W_{M-2}^n) + f_{\alpha((M-1/2)\,\Delta x)}(W_{M-1}^n)\right)$$

$$\left. +\frac{1}{2}\,sgn(A_{\alpha,\rho,u((M-1/2)\,\Delta x)})\,\left(f_{\alpha((M-1/2)\,\Delta x)}(W_{M-1}^n) - f_{\alpha((M-3/2)\,\Delta x)}(W_{M-2}^n)\right) \right\},$$

where f^+ is sought under the form:

$$f^+ = f_{\alpha((M-1/2)\,\Delta x)}(W_{M-1}^n) + \varepsilon_1\,\mathbf{r}_1 + \varepsilon_2\,\mathbf{r}_2,$$

and

$${}^t\mathbf{l}_2\,f^+ = {}^t\,\mathbf{l}_2\,f_{\alpha((M-1/2)\,\Delta x)}(W_{M-1}^n), \qquad f_2^+ = (f_1^+)^2/(\alpha\,p^{-1}(p_{out})) + \alpha\,p_{out}.$$

This leads to $\varepsilon_2 = 0$ and

$$f_{2;\alpha((M-1/2)\,\Delta x)}(W_{M-1}^n) - \varepsilon_1\,\frac{u-c}{2c}$$

$$= \frac{1}{\alpha\,p^{-1}(p_{out})}\,(f_{1;\alpha((M-1/2)\,\Delta x)}(W_{M-1}^n) - \frac{\varepsilon_1}{2c})^2 + \alpha\,p_{out}.$$

We take the smallest root ε_1 of the previous equation, that is

$$\varepsilon_1 = 2\,c^2\,\min\left(-\alpha\,p^{-1}(p_{out})\,\frac{u-c}{2c} + \frac{f_{1;\alpha((M-1/2)\,\Delta x)}(W_{M-1}^n)}{c} + \sqrt{\Delta}),\right.$$

$$\left. -\alpha\,p^{-1}(p_{out})\,\frac{u-c}{2c} + \frac{f_{1;\alpha((M-1/2)\,\Delta x)}(W_{M-1}^n)}{c} - \sqrt{\Delta})\right),$$

with

$$\Delta = \left(\alpha\,p^{-1}(p_{out})\,\frac{u-c}{2c} - \frac{f_{1;\alpha((M-1/2)\,\Delta x)}(W_{M-1}^n)}{c}\right)^2$$

$$-\frac{1}{c^2}\left(f_{1;\alpha((M-1/2)\,\Delta x)}(W^n_{M-1})^2+\alpha\, p^{-1}(p_{out})(-f_{2;\alpha((M-1/2)\,\Delta x)}(W^n_{M-1})+\alpha\, p_{out})\right).$$

Fourth step, third part: The sources (which do not appear in the mass equation) are treated with a centered explicit scheme:

$$W^{n+1}_{m(1)} = W^{n+1/2}_{m(1)},$$

$$W^{n+1}_{m(2)} = W^{n+1/2}_{m(2)} - \frac{R\,\Delta t}{\Delta x}\sum_{k\in L_m((n+1)\,\Delta t)}\mathcal{F}$$

$$\times\left(u((n+1/2)\,\Delta t,(m+1/2)\Delta x) - v_{k1}((n+1)\,\Delta t)\right)$$

$$+\Delta t\, p((n+1/2)\,\Delta t,(m+1/2)\Delta x)$$

$$\times\left(\frac{\alpha((n+1)\,\Delta t,(m+3/2)\Delta x)-\alpha((n+1)\,\Delta t,(m-1/2)\Delta x)}{2\,\Delta x}\right).$$

The last term in the force is slightly modified (un-centered) for the first and the last cell of the domain. At the end of the third part of the fourth step, we obtain the quantities $\rho((n+1)\,\Delta t,(m+1/2)\Delta x)$ and $u((n+1)\,\Delta t,(m+1/2)\Delta x)$.

Fifth step: The pressure is computed thanks to the pressure law:

$$p((n+1)\,\Delta t,(m+1/2)\Delta x) = C_0\,[\rho((n+1)\,\Delta t,(m+1/2)\Delta x)]^\gamma.$$

At the end of the fifth step, all the quantities x_k, v_k, $\rho(\cdot,(m+1/2)\Delta x)$, $u(\cdot,(m+1/2)\Delta x)$, $p(\cdot,(m+1/2)\Delta x)$, $\alpha(\cdot,(m+1/2)\Delta x)$ are known at the time $(n+1)\,\Delta t$, and the next time step of the numerical scheme can be performed.

In next section, we show results obtained thanks to the numerical scheme described above. In order to present results which are relevant for typical design cases, we consider a curved pipe rather than a straight pipe.

4 Numerical results

We now present a typical computation for a spray in a curved pipe, thanks to an adaptation of the scheme described in the previous section to a set of equations taking into account the curvature. We detail this set of equations below.

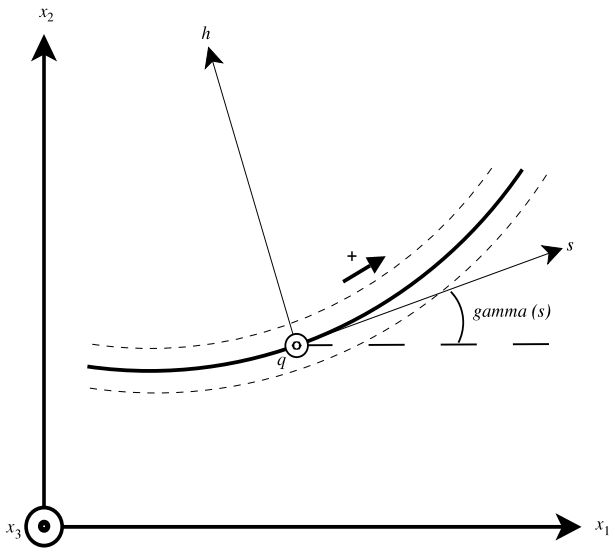

Figure 1. Geometry of the pipe

4.1 Establishment of the equations in a curved pipe

We first present the modifications to the equations (10) – (15) when one considers a pipe (of constant diameter D) with curvature (but without torsion: the center guide of the pipe is supposed to be contained in a vertical plane). The geometry of the pipe is described in figure 1

In order to get the equations for such a curved pipe, we introduce a change of variables in equations (1) – (6), defined as $(x_1, x_2, x_3) \mapsto (s, h, q)$, with

$$x_1 = \int_0^s \cos(\gamma(\sigma))\, d\sigma - h\, \sin(\gamma(s)), \quad x_2 = \int_0^s \sin(\gamma(\sigma))\, d\sigma + h\, \cos(\gamma(s)),$$

$$x_3 = q,$$

where s is the curvilinear variable along the center guide of the pipe, h is an orthogonal variable included in the vertical plane, and γ is the angle with the horizontal axis at a given point of the centerline of the pipe. Finally, we denote by q a variable orthogonal to the vertical plane in which the center guide of the pipe is included.

Note that this change of variables makes sense when $\frac{D}{2}\,|\gamma'(s)| < 1$: we shall systematically make this assumption in the sequel. We also introduce the veloc-

ity of the gas in the new reference frame, and its components:

$$\begin{cases} u_s = \cos(\gamma(s))\, u_1 + \sin(\gamma(s))\, u_2, \\ u_h = -\sin(\gamma(s))\, u_1 + \cos(\gamma(s))\, u_2, \\ u_q = u_3, \end{cases}$$

and for the droplets :

$$v_s = \cos(\gamma(s))\, v_1 + \sin(\gamma(s))\, v_2, \quad v_h = -\sin(\gamma(s))\, v_1 + \cos(\gamma(s))\, v_2, \quad v_q = v_3.$$

Introducing now the unknowns $\rho_s = \rho\,(1 - h\,\gamma'(s))$, and $f_s = f\,(1 - h\,\gamma'(s))$, equations (1) – (6) become

$$\partial_t(\alpha\,\rho_s) + \partial_s\left(\frac{\alpha\,\rho_s\,u_s}{1 - h\,\gamma'(s)}\right) + \partial_h(\alpha\,\rho_s\,u_h) + \partial_q(\alpha\,\rho_s\,u_q) = 0; \tag{23}$$

$$\partial_t(\alpha\,\rho_s\,u_s) + \partial_s\left(\frac{\alpha\,\rho_s\,u_s^2}{1 - h\,\gamma'(s)}\right) + \frac{1}{1 - h\,\gamma'(s)}\partial_h((1 - h\,\gamma'(s))\alpha\,\rho_s\,u_s\,u_h) \tag{24}$$

$$+\partial_q(\alpha\,\rho_s\,u_s\,u_q) + \frac{\partial p}{\partial s} = -\int_{v\in\mathbf{R}^3}\int_{r\in\mathbf{R}_+} f_s\,F_s\,dr dv - \alpha\,\rho_s\,|g|\,\sin(\gamma(s));$$

$$\partial_t f_s + v_s\,\frac{\partial}{\partial s}\left(\frac{f_s}{1 - h\,\gamma'(s)}\right) + v_h\,(1 - h\,\gamma'(s))\,\frac{\partial}{\partial h}\left(\frac{f_s}{1 - h\,\gamma'(s)}\right) + v_q\,\frac{\partial f_s}{\partial q} \tag{25}$$

$$+\frac{\gamma'(s)}{1 - h\,\gamma'(s)}\,v_s\left(v_h\,\frac{\partial f_s}{\partial v_s} - v_s\,\frac{\partial f_s}{\partial v_h}\right) + \frac{\partial}{\partial v_s}\left(f_s\left[\frac{F_s}{\frac{4}{3}\,\rho_l\,\pi\,r^3} - |g|\,\sin(\gamma(s))\right]\right)$$

$$+\frac{\partial}{\partial v_h}\left(f_s\left[\frac{F_h}{\frac{4}{3}\,\rho_l\,\pi\,r^3} - |g|\,\cos(\gamma(s))\right]\right) + \frac{\partial}{\partial v_q}\left(f_s\,\frac{F_q}{\frac{4}{3}\,\rho_l\,\pi\,r^3}\right) =$$

$$\int_{v*\in\mathbf{R}^3}\int_{r*\in\mathbf{R}_+}\int_{\theta=0}^{\pi}\int_{\phi=0}^{2\pi}\left(f_s(t,s,v',r)\,f_s(t,s,v^{*'},r^*) - f_s(t,s,v,r)\,f_s(t,s,v^*,r^*)\right)$$

$$\times\,\frac{B\left(\theta, \left|\begin{pmatrix} v_s - v_s^* \\ v_h - v_h^* \\ v_q - v_q^* \end{pmatrix}\right|, r, r^*\right)}{1 - h\,\gamma'(s)}\,d\theta d\phi dr^* dv^*;$$

where $v' = \begin{pmatrix} v'_s \\ v'_h \\ v'_q \end{pmatrix}$ and $v^{*'} = \begin{pmatrix} v^{*'}_s \\ v^{*'}_h \\ v^{*'}_q \end{pmatrix}$ are given by

$$v' = \frac{r^{*3}\begin{pmatrix} v^*_s \\ v^*_h \\ v^*_q \end{pmatrix} + r^3 \begin{pmatrix} v_s \\ v_h \\ v_q \end{pmatrix}}{r^{*3}+r^3} + \frac{r^{*3}}{r^{*3}+r^3} \left| \begin{pmatrix} v_s - v^*_s \\ v_h - v^*_h \\ v_q - v^*_q \end{pmatrix} \right| \begin{pmatrix} \sigma_s \\ \sigma_h \\ \sigma_q \end{pmatrix},$$

$$v^{*'} = \frac{r^{*3}\begin{pmatrix} v^*_s \\ v^*_h \\ v^*_q \end{pmatrix} + r^3 \begin{pmatrix} v_s \\ v_h \\ v_q \end{pmatrix}}{r^{*3}+r^3} - \frac{r^3}{r^{*3}+r^3} \left| \begin{pmatrix} v_s - v^*_s \\ v_h - v^*_h \\ v_q - v^*_q \end{pmatrix} \right| \begin{pmatrix} \sigma_s \\ \sigma_h \\ \sigma_q \end{pmatrix},$$

and with the force

$$F = \begin{pmatrix} F_s \\ F_h \\ F_q \end{pmatrix} = \mathcal{F}\Big(\frac{\rho_s}{(1-h\,\gamma'(s))}, r, \left| \begin{pmatrix} u_s - v_s \\ u_h - v_h \\ u_q - v_q \end{pmatrix} \right| \Big)$$

$$\times \begin{pmatrix} u_s - v_s \\ u_h - v_h \\ u_q - v_q \end{pmatrix} - \frac{4}{3}\,\pi\, r^3 \begin{pmatrix} \frac{1}{1-h\,\gamma'(s)}\,\frac{\partial p}{\partial s} \\ \frac{\partial p}{\partial h} \\ \frac{\partial p}{\partial q} \end{pmatrix}.$$

Note that the conservation of volume and pressure law now become

$$1 - \alpha = \int_{v\in\mathbf{R}^3} \int_{r\in\mathbf{R}} \frac{f_s}{1-h\,\gamma'(s)}\,\frac{4}{3}\,\pi\, r^3\, dr dv, \tag{26}$$

and

$$p = C_0 \left(\frac{\rho_s}{1-h\,\gamma'(s)} \right)^{\gamma}. \tag{27}$$

We then take the average of the equation over sections of the pipe (that is, part of the pipe for which s is a given number: it consists in integrating over h and q in $B(0, D/2)$ and dividing by $|B(0, D/2)|$), and we identify averages of nonlinear functions of the unknowns with nonlinear functions of these averages. Moreover, we impose that $u_h = u_q = 0$.

We introduce the quantity $\delta := \delta(s)$ which is the average of $(1 - h\,\gamma'(s))^{-1}$:

$$\delta(s) = \frac{4}{\pi\, D^2} \int_{B(0,D/2)} \frac{1}{1-h\,\gamma'(s)}\, dh dq,$$

and we keep the notations ρ_s, u_s, f_s, p for the averaged quantities.

Our set of equations becomes:

$$\partial_t(\alpha\,\rho_s) + \partial_s(\alpha\,\rho_s\,u_s\,\delta) = 0; \tag{28}$$

$$\partial_t(\alpha\,\rho_s\,u_s) + \partial_s(\alpha\,\rho_s\,u_s^2\,\delta) + \partial_s(\alpha\,p) = -\int_{v\in\mathbf{R}^3}\int_{r\in\mathbf{R}} f_s\,F_s^*\,dr dv \tag{29}$$

$$+p\,\partial_s\alpha - \alpha\,\rho_s\,|g|\,\sin(\gamma);$$

$$\partial_t f_s + \partial_s(v_s\,\delta\,f_s) + \partial_{v_s}\left(\left[\gamma'\,\delta\,v_h\,v_s + \frac{F_s}{\frac{4}{3}\,\rho_l\,\pi\,r^3} - |g|\,\sin(\gamma)\right] f_s\right) \tag{30}$$

$$+\partial_{v_h}\left(\left[-\gamma'\,\delta\,v_s^2 + \frac{F_h}{\frac{4}{3}\,\rho_l\,\pi\,r^3} - |g|\,\cos(\gamma)\right] f_s\right) + \partial_{v_q}\left(\frac{F_q}{\frac{4}{3}\,\rho_l\,\pi\,r^3}\,f_s\right) =$$

$$\delta\int_{v*\in\mathbf{R}^3}\int_{r*\in\mathbf{R}_+}\int_{\theta=0}^{\pi}\int_{\phi=0}^{2\pi}\left(f_s(t,s,v',r)\,f_s(t,s,v^{*'},r^*) - f_s(t,s,v,r)\,f_s(t,s,v^*,r^*)\right)$$

$$\times\,B\left(\theta,\left|\begin{pmatrix} v_s - v_s^* \\ v_h - v_h^* \\ v_q - v_q^* \end{pmatrix}\right|, r, r^*\right) d\theta d\phi dr^* dv^*;$$

with

$$F^* = \begin{pmatrix} F_s^* \\ F_h^* \\ F_q^* \end{pmatrix} = \mathcal{F}\left(\rho_s\,\delta, r, \left|\begin{pmatrix} u_s - v_s \\ -v_h \\ -v_q \end{pmatrix}\right|\right)\begin{pmatrix} u_s - v_s \\ -v_h \\ -v_q \end{pmatrix};$$

$$F = F^* - \frac{4}{3}\,\pi\,r^3\,\delta\begin{pmatrix} \frac{\partial p}{\partial s} \\ 0 \\ 0 \end{pmatrix};$$

$$1 - \alpha = \delta\int_{v\in\mathbf{R}^3}\int_{r\in\mathbf{R}} f_s\,\frac{4}{3}\,\pi\,r^3\,dr dv; \tag{31}$$

$$p = C_0\,(\rho_s\,\delta)^\gamma. \tag{32}$$

The set of equations (28) – (32) is then discretized with a variant of the scheme presented in section 3 (when the pipe is straight, the scheme is exactly the one which is presented in section 3).

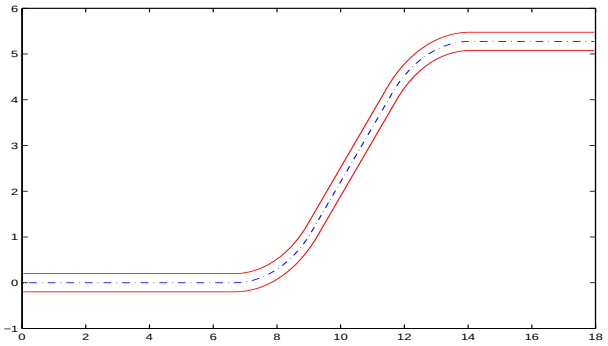

Figure 2. First test case: geometry of the pipe

4.2 Typical numerical experiences

We present here two typical simulations for a spray in a curved pipeline, modeled by eq. (28) – (32), and discretized by a variant of the scheme presented in section 3.

For each simulation, we show (at all points of the curvilinear variable $s \in [0, L]$) the time evolution of the pressure p, the volume fraction α (of gas) and the mean velocity of the liquid defined as $u_l = \frac{\int f v r^3 dv dr}{\int f r^3 dv dr}$ (and replaced by 0 when $f = 0$).

4.2.1 First test case

We chose a curved pipeline with the geometry described in figure 2. The length of the pipe is $L = 20.0$. All data are written in the International System of Units (SI).

The initial datum is homogeneous in space and without droplets :

$$\rho_s = 1.0 \qquad u_s = 100.0 \qquad f_s = 0.0.$$

The boundary conditions are chosen as follows :

$$G_{in} = 100.0 \qquad p_{out} = 80000.0,$$

with the density of the entering droplets given by :

$$\psi_+(t, v, r) = 2.10^5 \delta_{v=250.0} 1_{r\in[0.01,0,02]}.$$

The other constants and parameters of the model in this test are : the density of the liquid $\rho_l = 1100.0$, the pressure law in the gas $p = 100000.0\rho_g^{1.4}$, and the (constant) drag force coefficient $\phi_{lg} = 0.00001$.

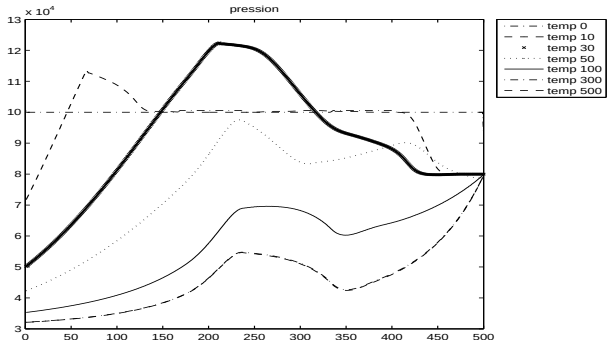

Figure 3. First test case: pressure at different times

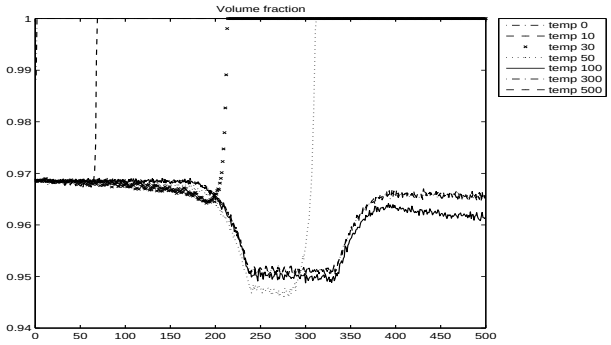

Figure 4. First test case: volume fraction at different times

The discretization parameters are the following: The representativity of the droplets is $R = 0.01$; the time step is $\Delta t = 0.00006$; the length step is $\Delta x = 0.04$.

The evolution of the pressure, volume fraction (of gas), and mean velocity of the droplets are respectively shown in figures 3, 4 and 5. The curves represent those quantities in terms of the space (curvilinear variable s) at records: 0; 10; 30; 50; 100; 300; 500. Note that one record is performed every 20 time steps (that is, every $1.2\,10^{-3}$ units of time).

4.2.2 Second test case

The parameters of the model and discretization are the same as in the first test case, but the pipeline has a steeper geometry described in figure 6.

The evolution of the pressure, volume fraction (of gas), and mean velocity of the droplets are respectively shown in figures 7, 8 and 9. The curves represent

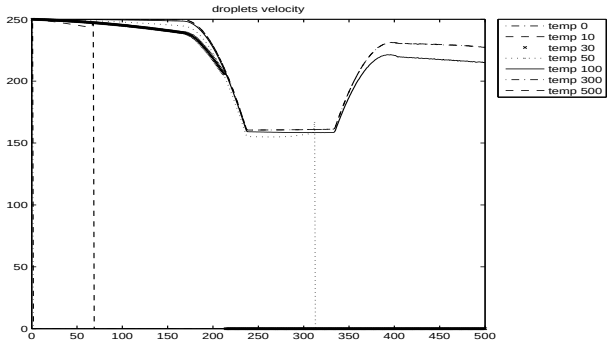

Figure 5. First test case: velocity of droplets at different times

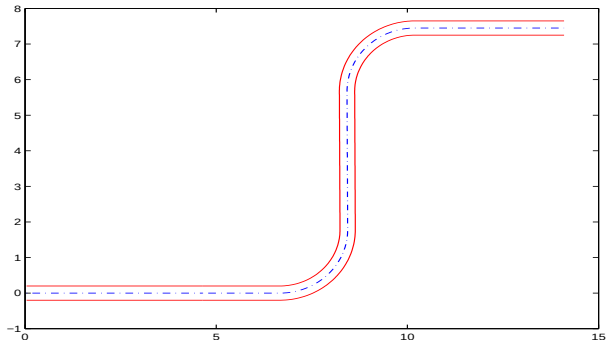

Figure 6. Second test case: geometry of the pipe

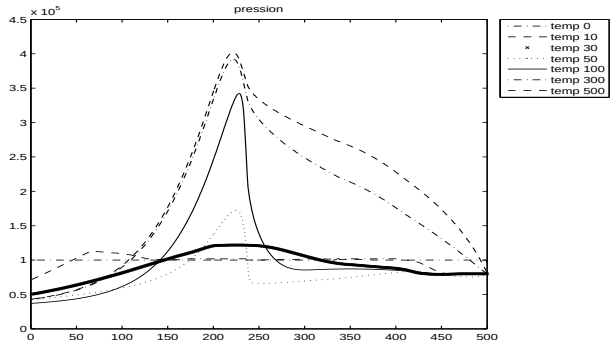

Figure 7. Second test case: pressure at different times

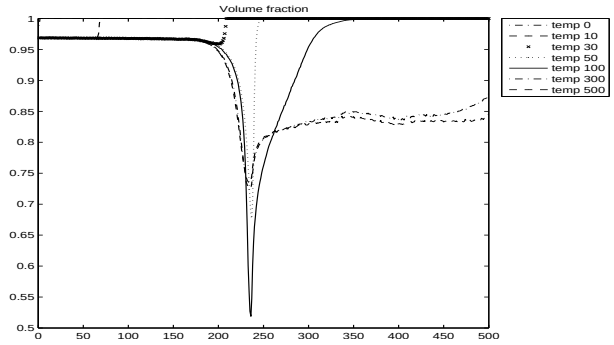

Figure 8. Second test case: volume fraction at different times

those quantities in terms of the space (curvilinear variable s) at the time: 0; 10; 30; 50; 100; 300; 500 records.

Other test cases will be presented in [2], together with extra precisions on the computation sketched here.

4.2.3 Comments on the two test cases

We first observe that the solution to our model seems to converge towards a steady solution, as can be seen by looking at the various curves at time steps 300 and 500. The transient is particularly complex due to propagation of waves in the pipe.

The numerical scheme seems to be stable, though the volume fraction curves show a random noise which is typical of PIC-DSMC methods.

As could be guessed, the pressure grows at the points where the pipe makes

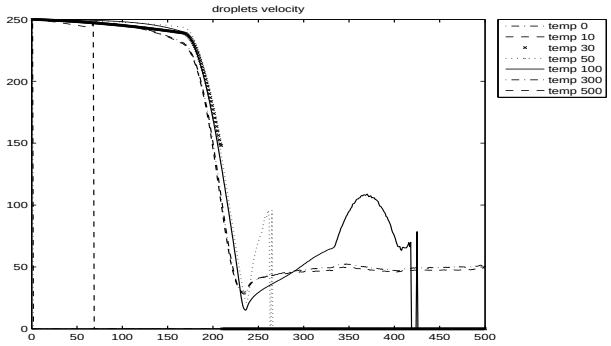

Figure 9. Second test case: velocity of droplets at different times

an angle with the horizontal line, while the volume fraction of gas and velocities of the droplets drop (droplets accumulate there).

As the curvature of the pipe increases (second test-case with respect to first test case), the pressure growth and the volume fraction/droplets velocity drop also increase. In the second test case, the volume fraction of droplets reaches values where the model is at the limit (and maybe gets out) of its validity.

4.3 A brief parametric study: Variation with respect to the angle of curvature

We finally present a brief parametric study, taking as parameter the slope of the pipeline.

We present the maximum pressure (in figure 10) and maximum volume fraction (in figure 11) of the steady state in function of the varying parameter (slope of the pipe) (in radians).

As can be seen, the process is far from linear. Note that when the angle is larger than 1.4, the model is at the limit of its validity.

4.4 Conclusions

The model and numerical scheme presented here seem to be robust: not too big oscillations are appearing in the simulations, even in computations in which the model is at the limit of its validity (large volume fraction of droplets, important curvature of the pipe).

While performing the simulations, we noticed that this robustness is slightly lessened when the model is discretized in such a way that the source term is not $p\,\partial_x\alpha$ any more: this can be understood since the pure gas case corresponds to

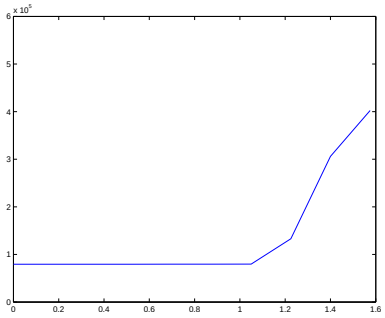

Figure 10. Maximum pressure w.r.t slope of the pipe

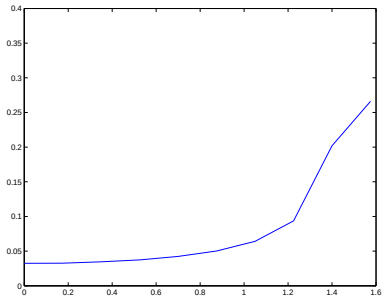

Figure 11. Maximum volume fraction w.r.t slope of the pipe

$\alpha = 1$, where one recovers the usual flux for Euler's equation in (16).

We also noticed that the collisions do not have an important effect on the physical macroscopic outputs. They however provide a slightly smoothing effect on the oscillations of the volume fraction profile.

Acknowledgements. This work has been partially supported by the French national research agency (ANR) grant ANR-10-BLAN-1119-02 SAMOVAR.

References

[1] Arkeryd L., Cercignani C. and Illner R., *Measure solution of the steady Boltzmann equation in a slab*, Commun. Math. Phys., **142**, (1991), 285-296.

[2] Benjelloun S. PhD thesis, ENS Cachan, France, in preparation.

[3] Baranger C. and Desvillettes L., *Coupling Euler and Vlasov equations in the context of sprays: the local-in-time, classical solutions*, J. Hyperbolic Differ. Equ., **3**, n.1, (2006), 1-26.

[4] Boudin L., Desvillettes L. and Motte R., *A Modeling of Compressible Droplets in a Fluid*, Commun. Math. Sci., **1**, n.4, (2003), 657-669.

[5] Bird G. A., Molecular Gas Dynamics and the Direct Simulation of Gas Flows, Claredon, Oxford, 1994.

[6] Baranger C. Modélisation, étude mathématique et simulation des collisions dans les fluides complexes. PhD thesis, ENS Cachan, France, 2004.

[7] Desvillettes L., *Some Aspects of the Modeling at Different Scales of Multiphase Flows*, Comput. Meth. Appl. Mech. Engineering, **199**, (2010), 1265-1267.

[8] Faghri A. and Zhang Y., Transport phenomena in multiphase systems, Academic Press, 2006.

[9] Godlewski E. and Raviart P.A., Numerical Approximation of Hyperbolic Systems of Conservation Laws. Springer, New-York, 1996.

[10] Ghidaglia J.-M., Kumbaro A. and Le Coq G., *Une méthode volumes finis à flux caractéristiques pour la résolution numérique des systèmes hyperboliques de lois de conservation*, C. R. Acad. Sc. Paris I, **322**,(1996), 981-988.

[11] Ghidaglia J.-M., Kumbaro A. and Le Coq G., *On the numerical solution to two fluid models via a cell centered finite volume method*, Europ. Journal Mech. B/Fluids, **20**, (2001), 841-867.

[12] Grigoryev Yu.N., Vshivkov V.A. and Fedoruk M.P., Numerical Particle-in-Cell Methods - Theory and Applications. VSP BV, Utrecht, 2002.

[13] Ishii M. and Hibiki T., Thermo-Fluid Dynamics of Two-Phase Flow, Springer, New-York, 2006.

[14] LeVeque R. J., Numerical methods for conservation laws, 2^{nd} edition, Lectures in Mathematics, ETH Zürich, Birkhäuser Verlag, Basel, 1992.

[15] Pareschi L., Monte Carlo Methods for Kinetic Equations, Quantum and Kinetic Transport: Tutorials, IPAM - UCLA, USA, march 10-13, 2009.

[16] Mathiaud J. Etude mathématique et numérique des systèmes de type gaz-particules, PhD Thesis, ENS Cachan, France, 2006.

[17] O'Rourke P. J., Collective drop effects on vaporizing liquid sprays. PhD Thesis, Los Alamos National Laboratory, 1981.

[18] Williams F. A., Combustion theory, 2^{nd} edition, Benjamin Cummings, 1985.